International Journal of Advances in Engineering and Management (IJAEM)
Volume 3, Issue 12 Dec 2021, pp: 1262-1274 www.ijaem.net ISSN: 2395-5252

Supervision of Electric Power Generation Units by a Multivariable Neural System

G. Ramanantena[1], E. Randriamora[2], E. Rastefano[3]

[1]*Ph.D Student in Electrical Engineering, Ecole Doctorale en Sciences et Techniques de l'Ingénierie et de l' Innovation (ED-STII), University of Antananarivo, Antananarivo, Madagascar.*
[2]*Thesis Co-Director, ED-STII, University of Antananarivo, Antananarivo, Madagascar.*
[3]*Thesis Director, ED-STII, University of Antananarivo, Antananarivo, Madagascar.*
Corresponding Author: Gilbert Ramanantena,

Date of Submission: 10-12-2021 Revised: 20-12-2021 Date of Acceptance: 25-12-2021

ABSTRACT: Supervision of electric power generation systems has been carried out either by model predictive control or by fuzzy logic in the literature. This paper proposed the new supervision for electric power generation units connected to the interconnected power system. This new method was based on the artificial neural networks. The architecture of the artificial neural networks supervisor obtained using the neural network toolbox under Matlab was (5-7-4). The results obtained showed that this artificial neural networks supervisor was able to participate in the secondary frequency control in mode automatic.

KEYWORDS: artificial neural networks (ANN) supervisor, Diesel power plants (DPP), hydroelectric power plants (HPP), proportional integral (PI) controller, secondary frequency control (SFC).

I. INTRODUCTION

Frequency stability of Electric Power System (EPS) consists in achieving a balance, at all times, between the production and the consumer. Maintaining this balance therefore requires a permanent supervision system to ensure the stability of this EPS. In the literature, there are three types of supervision used to manage Electric Power Generation (EPG) Systems (a) Model Predictive Control (MPC)-based supervision (b) Fuzzy Logic (FL) supervision (c) Artificial Neural Network-based supervision. The work of Negenborn et al (2007) studies the voltage stability of the 9 bus power system, called the Anderson-Farmer power system, using a monitoring system based on MPC [1]. They (2009) also study voltage control for the 9-bus power system through the use of nonlinear MPC supervision using pattern search [2]. Qi et al (2011) create a MPC supervisor to provide the reference power of Solar-Wind Generators for an isolated grid [3]. Tedesco et al (2016) propose the supervision of the microgrid by the approach of a MPC. The goal of their work is to optimize the power flow in real time [4]. The research work of Courtecuisse et al (2007), develop the supervision strategy based on FL for a Hybrid Generator. This supervisor proposed by the authors made it possible to maintain the reference power and to contribute to the Primary Frequency Control (PFC) and Secondary Frequency Control (SFC) settings [5]. Boukettaya et al (2007) create a Fuzzy Logic Supervisor (FLS) to control the powers generated from a Hybrid Power Generation Unit [6]. Herbreteau et al (2008) study the FL-based supervision strategy for Hybrid Generation Systems (HGSs) connected to the power grid in order to improve the integration of Dispersed Generators [7]. Li et al (2009) are interested in the participation of the PFC and SFC of a resident microgrid connected to the radial distribution using a FLS [8]. Nasser et al (2011) propose a FLS for Hybrid Renewable Energy Systems (HRESs) composed of Wind Turbine, Hydroelectric Power Plant and Storage System connected to the AC grid [9]. The work of Shabib (2012) studies the application of FLS with a PID (Proportional-Integral-Derivator) controller for an excitation system of a generator connected to the infinite bus [10]. The work of Ngoffe et al (2016) present the method of optimizing a FLS applied to the HRES consisting of three Diesel Generators, an Energy Storage Unit (supercapacitor) and a Photovoltaic Generator [11]. Krim et al (2017) propose the control and a FLS for a wind power system associated with a Hybrid Energy Storage System (batteries and supercapacitor) connected to the power grid [12]. Roumila et al (2017) develop an intelligent supervisor based on Fuzzy Logic Control (FLC) for HGSs composed of Wind Turbine, Diesel Generator, Photovoltaic and Storage

International Journal of Advances in Engineering and Management (IJAEM)
Volume 3, Issue 12 Dec 2021, pp: 1262-1274 www.ijaem.net ISSN: 2395-5252

Batteries [13]. The work of Chaouali et al (2018) is interested in the management of HRESs composed of Photovoltaic, a Proton Exchange Membrane Fuel Cell (PEMFC) for a water pumping station in an isolated grid [14]. As for supervision based on Artificial Neural Networks (ANN), Mohagheghi et al (2005) develop an ANN supervisor for multimachines and a FACTS device in an EPS. This proposed supervisor sends control signals in the form of reference power to the multimachines and the reference voltage to the FACTS device [15]. It should be noted that Younci et al (2011), they develop a supervisor using ANN for the optimum operation of Hybrid Renewable Energy Generators (Wind Generator, Diesel Generator and Flywheel Energy Storage System). This proposed supervisor makes it possible to supply the reference power to the HREGs [16]. Lu (2019) proposes the control of a power converter which is associated with the Virtual Synchronous Generator connected to the EPS. The goal of the author is to improve the frequency nadir of this studied system [17]. The work of Morovati and Painemal (2021) proposes a novel coordinating mechanism between Synchronous Generators and Wind Turbines (WTs) based on Doubly Fed Induction Generators (DFIGs) for enhanced PFC. In this case, ANN is used to obtain an optimal coordination signal to improve frequency response [18]. So far no-one has studied ANN-based Electric Power Generation (EPG) supervision for SFC.

In this article, the main objective is to create the ANN supervisor for the EPG units connected to the interconnected power system in order to participate in the SFC. This supervisor sends control signals in the form of reference power to the controllers of these EPG.

II. MATERIALS AND METHODS

Used material in this section is shown below (Fig.1). It is an interconnected power system (IPS) of the region DIANA, named RIDIANA [19]. This material is made up of (a) three HPP (Ampandriambazaha has two 25 MW units, Andranomamofona has three 5 MW and Bevory consists of two 6 MW units) (b) five Diesel power plants (DPP) for the five districts (c) seven HV transmission lines including four 90 kV transmission lines and three 220 kV transmission lines (d) fifteen power transformers (e) five loads that are powered by DPP.

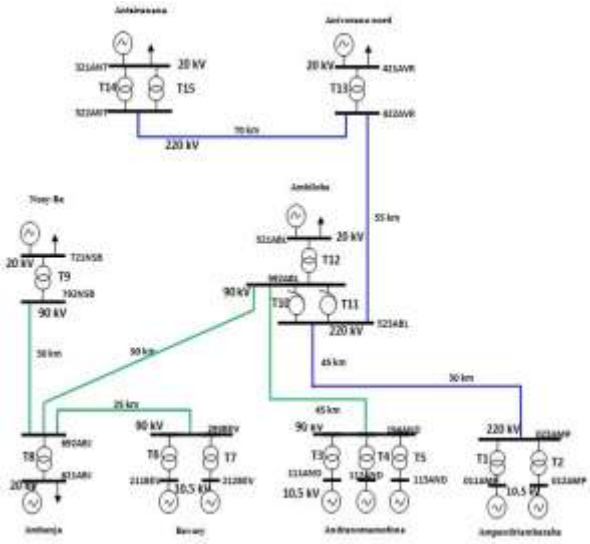

Fig.1: Interconnected power system of the region DIANA

2.1. Hydroelectric Generator (HG) model

Figure.2 shows the HG that makes up the (a) synchronous generator (SG) (b) the hydraulic turbine (HT) (c) the servomotor (d) the exciter (e) the speed governor (SGN) and (f) the automatic voltage regulator (AVR) [20]

International Journal of Advances in Engineering and Management (IJAEM)
Volume 3, Issue 12 Dec 2021, pp: 1262-1274 www.ijaem.net ISSN: 2395-5252

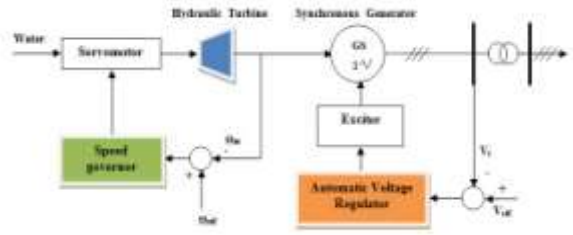

Fig.2: HG with its control systems

The following subsection relates only the models of the HT, the SGN and the AVR.

2.1.1. Hydraulic turbine model

The HT used in this paper is of the Francis type [19]. It is a device that converts potential energy of water into mechanical energy to drive a SG. The transfer function of HT is defined by

$$G_{HT}(s)=\frac{1-T_w.s}{1+0.5\times T_w s} \qquad (1)$$

with T_w is the hydraulic time constant in s.

2.1.2. Speed governor model

A speed governor is used to regulate the speed or the power supplied by the HT in the event of a variation the frequency of the electrical power system [21]. The figure below shows the principle of SGN

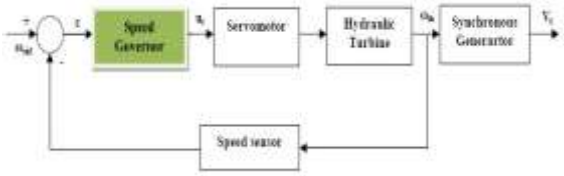

Fig.3: Principle of speed governor

For a Proportional Integral (PI) type SGN, its transfer function becomes

$$G_{SGO}(s)=\frac{\frac{1}{\delta_s}\times\left(1+\frac{K_p.s}{K_i}\right)}{1+\left(\frac{K_p}{K_i}+\frac{\delta_s}{K_i}\right).s} \qquad (2)$$

with K_p: SGN proportional gain, K_i: SGN integral gain, δ_s: droop.

The servomotor model is described by a simple first order transfer function similar to that of the motor

$$G_{SRV}(s)=\frac{K_s}{1+T_s.s} \qquad (3)$$

where K_s is the servomotor gain constant, T_s servomotor time constant in s.

2.1.3. Automatic voltage regulator model

The output of the AVR depends only the terminal voltage (V_t) of the SG [21]. It acts on the SG exciter to keep terminal voltage constant. Figure.4 shows the block diagram of the voltage the AVR on a SG [22]

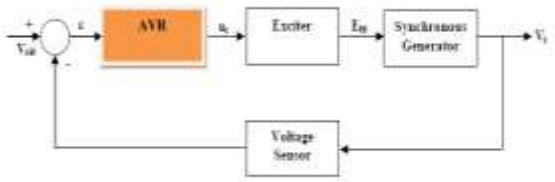

Fig.4: Principle of voltage regulation of HG

International Journal of Advances in Engineering and Management (IJAEM)
Volume 3, Issue 12 Dec 2021, pp: 1262-1274 www.ijaem.net ISSN: 2395-5252

The transfer equations for the block elements in Fig.4 are (a) for the AVR, its transfer function can be written [21]

$$G_{AVR}(s) = \frac{K_r}{1 + T_r.s} \qquad (4)$$

with K_r and T_r represent the AVR gain and time constant, respectively, in s
(b) for the exciter [21]

$$G_{EXC}(s) = \frac{1}{1 + T_e.s} \qquad (5)$$

with T_e: exciter time constant in s
(c) the transfer function of the SG is the ratio between the output voltage and the field voltage of this SG [21]

$$G_{SG}(s) = \frac{V_t}{E_{fd}} = \frac{K_g}{1 + T_g.s} \qquad (6)$$

where V_t: SG terminal voltage, E_{fd}: field voltage of the SG, K_g and T_g are SG gain and time constant, respectively.

2.2. Diesel Generator (DG) model

A DG is the combination of a Diesel engine (DE) with a Synchronous generator (SG) to generate electrical energy. The basic components of a DG are [23-24] (a) DE, (b) speed regulator (SR), exciter and SG. The following Fig.5 shows the block diagram of the DG [25]

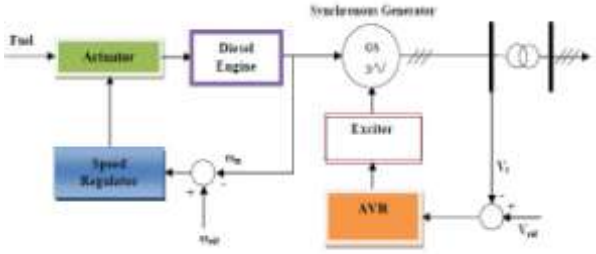

Fig.5: DG with its control systems

2.2.1. Diesel engine model

Diesel engine (DE) is the non-linear system. It is equipped with a SR. This automatically controls the speed of the DE by adjusting the fuel injection according to the load [26]. The following figure shows the functional structure of the speed control supplying the DE

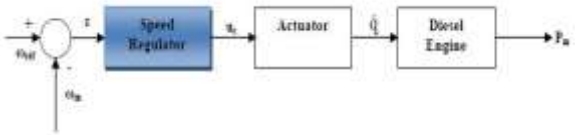

Fig.6: Functional diagram of the Diesel engine

The mechanical power supplied by the DE is

$$P_m = K_{mD}.e^{-\tau_{mD}.S}.\dot{q}.\omega_m \qquad (7)$$

where K_{mD} is the gain of the DE, $\dot{q}$ is the fuel mass flow in kg/s, ω_m is the angular speed of mechanical rotation of the DE expressed in rpm.

2.2.2. Speed regulator model

Figure.7 shows the Diesel engine (DE) drive system that can participate in frequency control [26-27]

International Journal of Advances in Engineering and Management (IJAEM)
Volume 3, Issue 12 Dec 2021, pp: 1262-1274 www.ijaem.net ISSN: 2395-5252

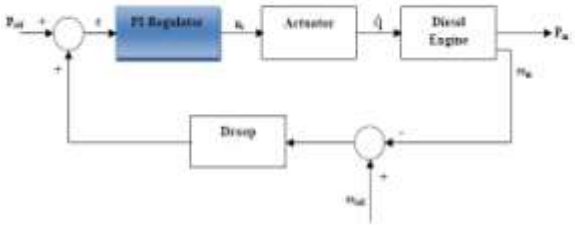

Fig.7: Diagram of the Diesel engine drive

The transfer function equations for the elements in Fig.7 are then written as follow
(a) the transfer function of the PI regulator can be written as

$$G_{SR}(s) = K_p.\left(1+\frac{1}{T_i.s}\right) \quad (8)$$

(b) the transfer function of the actuator which controls the fuel according to the output of the SR is modeled by

$$G_{AC}(s) = \frac{\dot{q}}{u_c} = \frac{K_{ac}}{1+\tau_{ac}.s} \quad (9)$$

with K_{ac} is the actuator gain constant, τ_{ac} is the actuator time constant in s;

(c) the Diesel engine (DE) follows the thermodynamic process law. So, it is modeled by:

$$G_{DE}(s) = K_{mD}.\left(\frac{1+\tau_{1mD}.s}{1+\tau_{2mD}.s}\right) \quad (10)$$

where K_{mD} is the DE gain constant, τ_{1mD} and τ_{2mD} are the time constants of the thermodynamic process of the DE in s.

2.2.3. Automatic regulator voltage model

The voltage regulation of the DG is carried out by an AVR acting of the SG exciter in order to provide the excitation voltage necessary to keep the alternating output voltage constant at its reference value. Fig.8 gives the block diagram of the Diesel generator excitation system [26], [28]

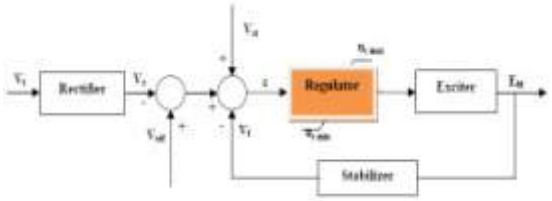

Fig.8: DG output voltage regulation

The transfer function equations for the block elements in Fig.8 are then written as follow
(a) the rectifier transfer function can be written in the form

$$G_{REC}(s) = \frac{1}{1+T_{red}.s} \quad (11)$$

with T_{red} is the rectifier time constant in s
(b) the regulator transfer function is given by [21]

$$G_{REG}(s) = \frac{K_r}{1+T_r.s} \quad (12)$$

(c) the exciter transfer function can be written as follow

$$G_{EXC}(s) = \frac{1}{K_e+T_e.s} \quad (13)$$

with K_e and T_e are the exciter gain and time constant, respectively;
(d) the stabilizer transfer function is of the following first order:

$$G_{STA}(s) = \frac{K_c.s}{1+\tau_c.s} \quad (14)$$

where K_c: stabilizer gain constant and T_c: stabilizer time constant in s.

2.3. Supervision strategy

Objective of this section is propose the supervision strategy that we have designed-based on an artificial neural networks (ANN) in [29-30] for

International Journal of Advances in Engineering and Management (IJAEM)
Volume 3, Issue 12 Dec 2021, pp: 1262-1274 www.ijaem.net ISSN: 2395-5252

the electric power generation (EPG) units connected to the interconnected power system (IPS) in order to participate in the secondary frequency control (SFC).

2.3.1. Structure of the interconnected electric system

Figure.9 shows the studied electrical system managed by an ANN supervisor [29-30]

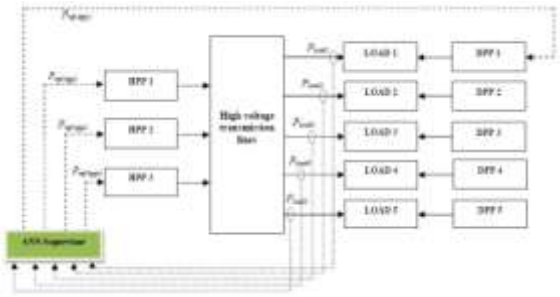

Fig.9: Structure of the interconnected electric system

This is mainly (a) an ANN supervisor (b) three hydroelectric power plants (HPPi, with $i=\overline{1,3}$) (c) five Diesel power plants (DPPj, with $j=\overline{1,5}$) (d) high voltage (HV) transmission lines to transport the electrical energy produced (e) five loads (LOADk, with $k=\overline{1,5}$) which are supplied by DPP.

2.3.2. Structure of the ANN supervisor

An ANN supervisor is a novel means of the processing information inspired by working of biological neurons. According to the study carried out in [29-30], the ANN supervisor is a multivariable neural system

Fig.10: Structure of the ANN supervisor

The different variables of the ANN supervisor are
(a) input variables: P_{loa1} represents the power measured at load n°1, P_{load2} which is the power measured at the second load, P_{load3} the measured power of load n°3, P_{load4} the power of the fourth load supplied by the DPP4, P_{load5} is the power measured at the load n° 5
(b) output variables: $P_{ref\text{-}dpp1}$ represents the reference power of the Diesel power plant (DPP1), $P_{ref\text{-}hpp1}$ represents the reference HPP1 power, $P_{ref\text{-}hpp2}$ is the reference power of the second power plant HPP2, $P_{ref\text{-}hpp3}$ is the reference power that drives HPP3.
This ANN supervisor works like a black-box. Based on the work done in [29-30], the size of the ANN configuration for the supervision of EPG units is (5-7-4). So, its architecture can be represented as follow

International Journal of Advances in Engineering and Management (IJAEM)
Volume 3, Issue 12 Dec 2021, pp: 1262-1274 www.ijaem.net ISSN: 2395-5252

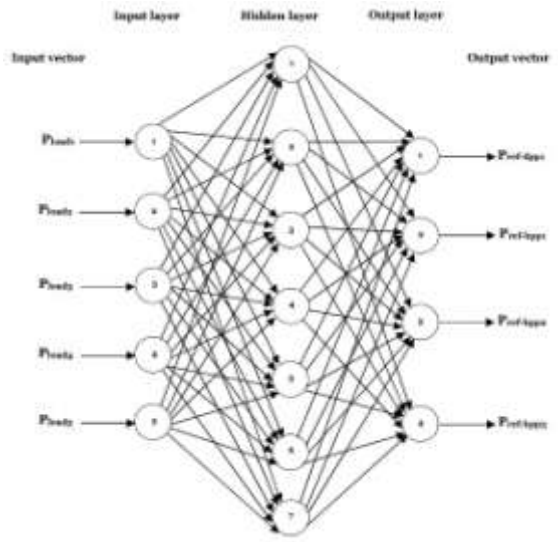

Fig.11: Structure of the ANN (5-7-4) architecture applied to supervision

2.3.3. Control strategy for EPG units by ANN supervisor

In this subsection, an intelligent control strategy for electric power generation (EPG) units is proposed. Each EPG unit connected to the electrical power system (EPS) has an internal control system that can participate in the primary frequency control (PFC) using the speed regulator. When there is excessive load (consumption) variation, EPG units fail to meet the balance between the production and consumption. In this case, there is no zero frequency deviation from the setpoint frequency of the EPS.

In order to participate in the SFC of the EPS studied, an ANN supervisor (or external) is necessary to guarantee coordination between the different EPG units connected to the EPS. To do this, this supervisor sends control signals in the form of reference powers to the different EPG units. The figure below illustrates the strategy for controlling EPG units using ANN supervisor

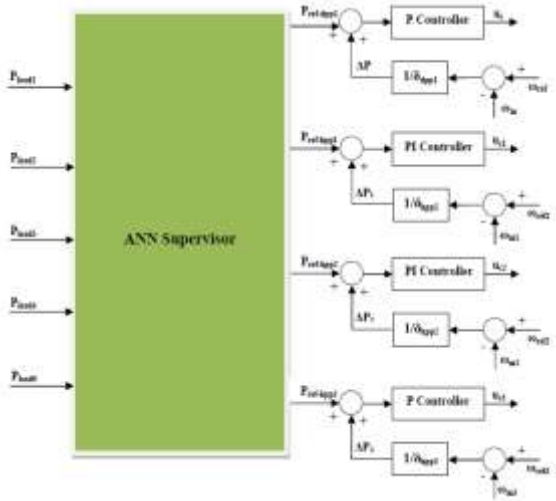

Fig.12: Control diagram of EPG units participating in frequency control

Figure.12 illustrates the principle of controlling EPG units using ANN supervisor. The latter should intervene at the instructions of the drive motor regulators of the HPPi, with $i=\overline{1,3}$ as well as the Diesel power plant type DPP1 according to load variations. In this case, the control law of the hydroelectric generator i, denoted $u_{ci}(s)$, make it possible to participate in the SFC. It can be defined as follows

$$u_{ci}(s)=G_{PI}(s)\left(P_{ref-hppi}+\frac{(\omega_{réfi}-\omega_{mi})}{\delta_{hppi}}\right) \quad (15)$$

International Journal of Advances in Engineering and Management (IJAEM)
Volume 3, Issue 12 Dec 2021, pp: 1262-1274 www.ijaem.net ISSN: 2395-5252

with $i = \overline{1,3}$ and for the case of the Diesel power plant DPP1 is

$$u_c(s) = G_{PI}(s).\left(P_{ref-dpp1} + \frac{(\omega_{réf} - \omega_m)}{\delta_{dpp1}} \right) \qquad (16)$$

with $G_{PI}(s)$ is the PI controller transfer function; $P_{ref\text{-}hpp\ i}$ is the reference power of HPPI, $P_{réf\text{-}dpp1}$: reference power of the DPP1 type Diesel power plant (DPP), $\omega_{réf\ i}$ is the angular speed of rotation of HPPi, expressed in rpm, ω_m: angular speed of mechanical rotation in rpm, $\delta_{hpp\ i}$ is the droop of HPPi and δ_{dpp1}: droop of DPP1.

III. RESULTS

To simulate the interconnected power system of the region DIANA, named RIDIANA, illustrated in Fig.1, we carried it out under Matlab software using Simulink and SimPowerSystems. Two types of simulations are presented (a) loads variation (b) short-circuits.

During the simulation, for two cases, the loads connected to the following bus were permanent (a) 21 MW at bus 321ANT (b) 0.343 MW for 421AVR (c) 2.5 MW for bus 521ABL (d) 5 MW at bus 621ABJ (e) 13.8 MW for bus 721NSB.

3.1. Loads variation

Fig.14 shows the frequency evolution of the four power plants (DPP1, HPP1, HPP2 and HPP3). And Fig.17 for the active power evolution supplied by the four power plants.

3.2. Short-circuits

Fig.15 shows the frequency evolution of the four power plants (DPP1, HPP1, HPP2 and HPP3) during short-circuits.

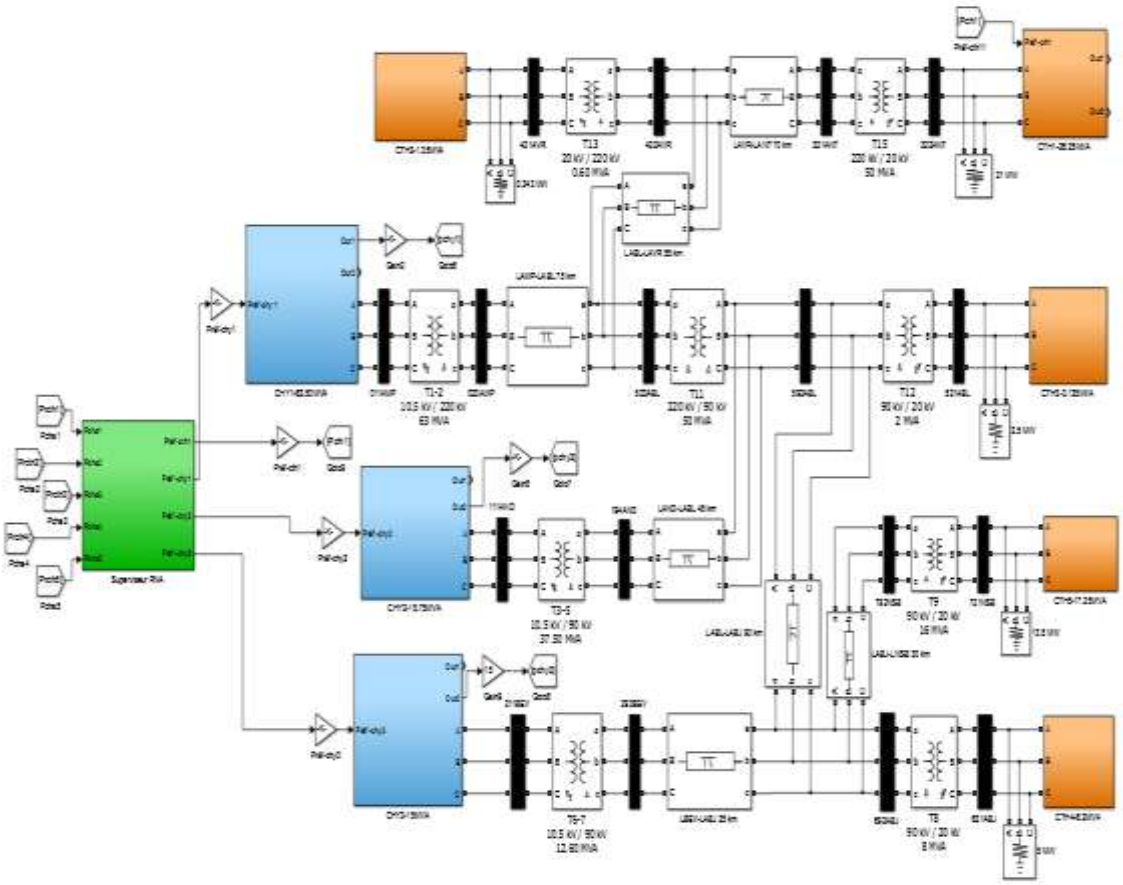

Fig.13: RIDIANA managed by ANN supervisor under Simulink

International Journal of Advances in Engineering and Management (IJAEM)
Volume 3, Issue 12 Dec 2021, pp: 1262-1274 www.ijaem.net ISSN: 2395-5252

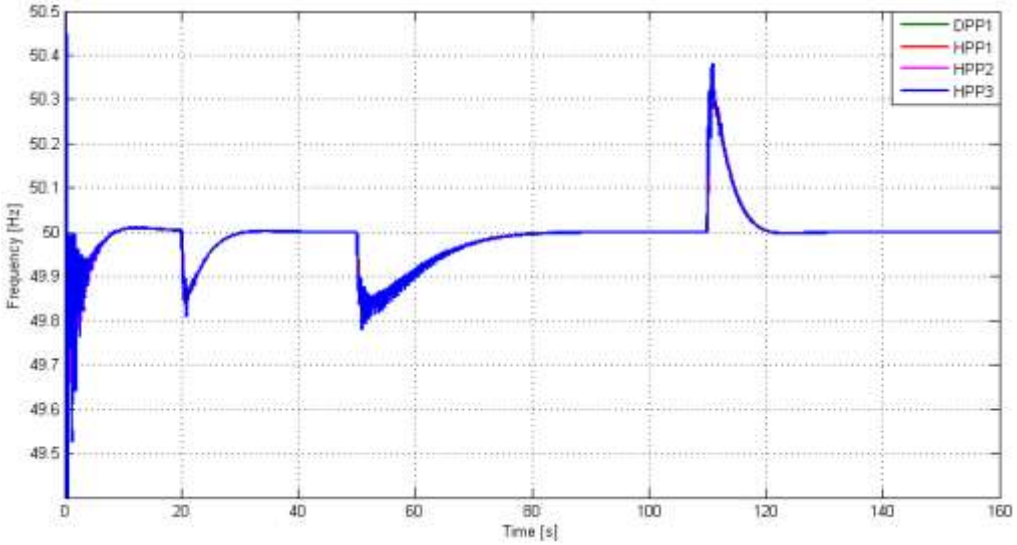

Fig.14: Frequency of RIDIANA during loads variation

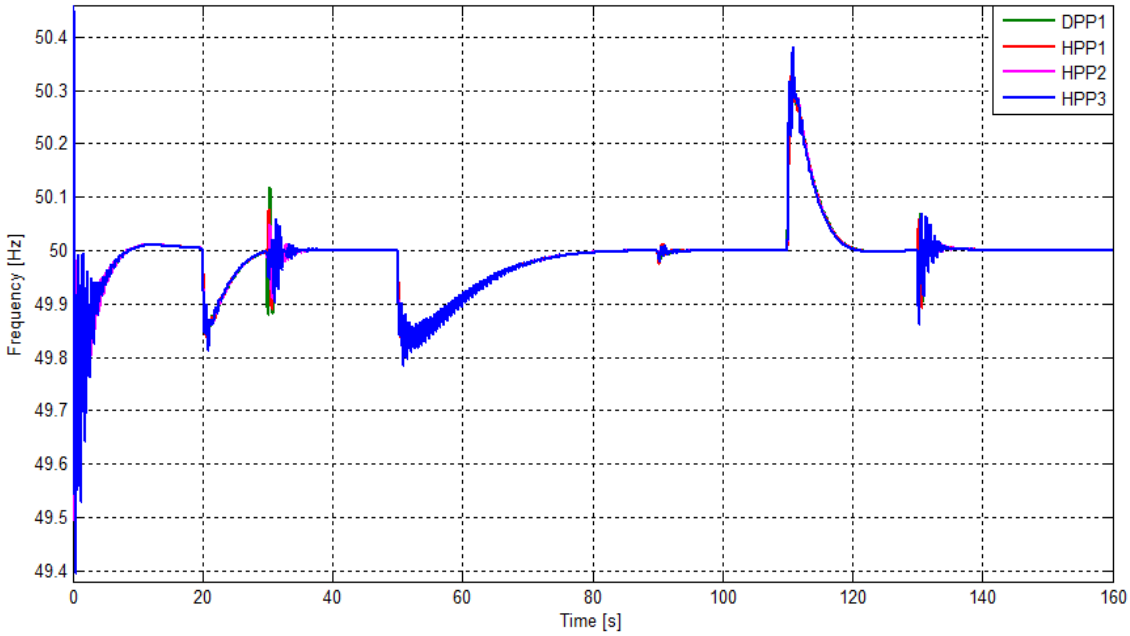

Fig.15: Frequency of RIDIANA during short-circuits

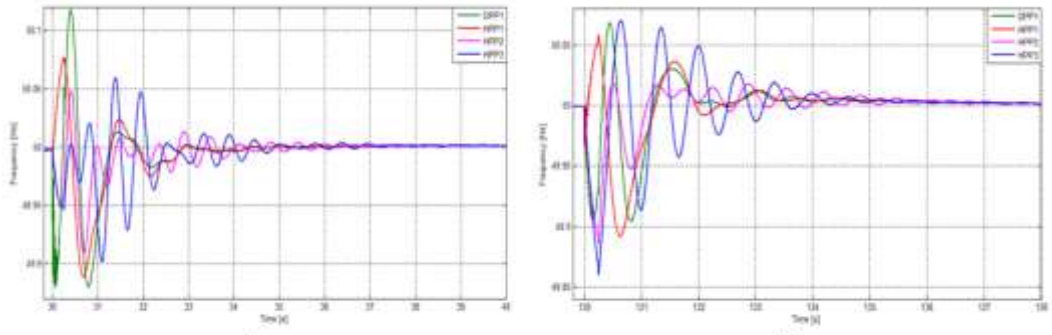

a) b)

International Journal of Advances in Engineering and Management (IJAEM)
Volume 3, Issue 12 Dec 2021, pp: 1262-1274 www.ijaem.net ISSN: 2395-5252

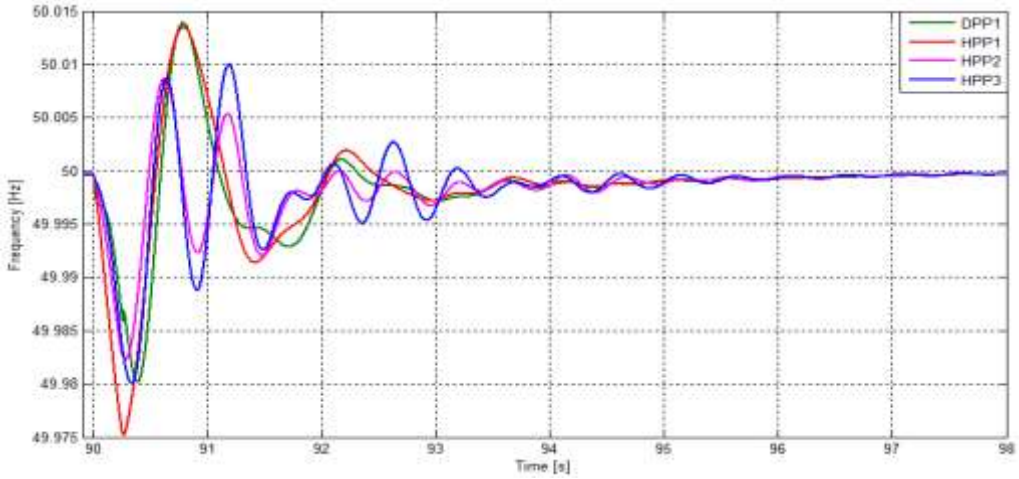

c)

Fig.16: Zoom the Frequency evolution of the RIDIANA

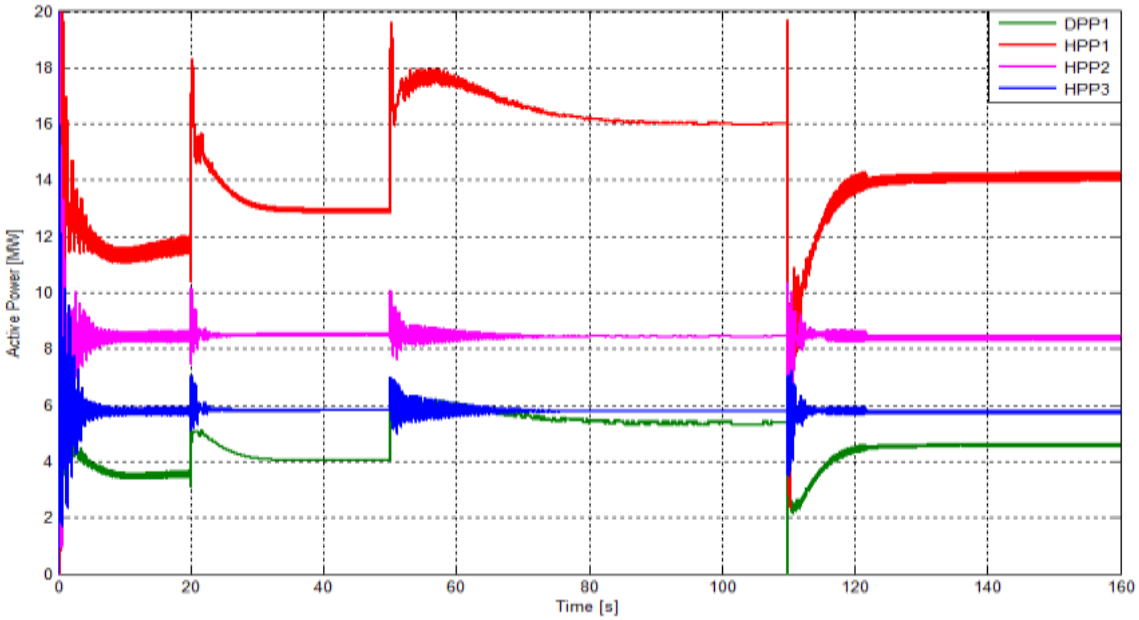

Fig.17: Active power evolution during loads variation

IV. DISCUSSION

Proposed ANN supervisor in this paper does participate in the secondary frequency control in automatic mode according to Fig.14 and Fig.15.

A sudden loads connection of 9.75 MW in total was caused at time t = 20 s at bus 321ANT, 621ABJ and 721NSB. Frequency of this RIDIANA has evolved from 50 Hz to 49.85 Hz. The transit of active power for the four power plants (DPP1, HPP1, HPP2 and HPP3) has increased by

(5.08 MW, 16.16 MW, 9.86 MW and 6.88 MW), respectively, so as to balance production and consumption according to Fig. 17. Oscillations of the active power appeared as a result of the abrupt connection of the loads. At

t = 32 s, the frequency value of the RIDIANA reached 50 Hz. Two power plants DPP1 and HPP1 participated in the SFC according to Fig. 17 and values active power were respectively 4 MW and 13.08 MW. A load variation of 10.25 MW was caused at time t = 50 s at buses 321ANT, 421AVR, 621ABJ and 721NSB. The frequency dropped from 50 Hz to 49.81 Hz. According to Fig. 17 two power plants DPP1 and HPP1 provided active power of 18 MW and 6.2 MW respectively. So, they participated in the SFC. On the other hand two power plants HPP2 and HPP3 only participated in the PFC. From the instant t = 85 s, the frequency of the RIDIANA became 50 Hz. It was noticed that the duration of the SFC were 35 s. So this power

system was stable. At t = 110 s, the loads (5 MW, 1.75 MW and 3 MW) at the buses (321ANT, 621ABJ and 721NSB) have respectively disconnected. According to Fig.17 the frequency value increased by 50.38 Hz. This is the phenomenon overproduction. After 11 s, the frequency became 50 Hz. So this RIDIANA became stable again.

Fig. 15 shows the frequency evolution of the RIDIANA during short-circuits in the three different parts. A first single-phase short-circuit, at t = 30 s, was carried out at the terminals of the Diesel power plant DPP1, with a fault clearing time of 250 ms. According to Fig. 16.a), the frequency of the power plant DPP1 made a large amplitude oscillation with respect to the three power plants (DPP1, HPP2 and HPP3). The maximum value of this frequency reached 50.12 Hz and the minimum were 49.88 Hz. This frequency became 50 Hz at 4.25 s after clearing the fault. A second single-phase short-circuit occurred in the middle of the 220 kV transmission line (between buses 322ANT and 422AVR) at t = 90 s. Following the disturbance, frequency oscillations of the same curve (Fig. 16.c)) were observed for the four power plants. These oscillations were damped at t = 95 s and the frequency value of the RIDIANA became 50 Hz. Therefore, this power system became stable. A third single-phase short-circuit made across the HPP1 at time t = 130 s. This fault were cleared at 250 ms. Frequency of the HPP1 dropped sharply from 50 Hz to 49.97 Hz. The amplitudes of the frequency oscillations of the four power plants were increasingly damped. At t = 138 s, the frequency value of this RIDIANA became 50 Hz. Therefore, this power system became stable again.

Results obtained, according to Fig.14 and Fig.15, are similar to the work carried out by Courtecuisse et al (2007) and by Li et al (2009) based on the FL supervisor concerning the participation of the Secondary Frequency Control [5], [8].

V. CONCLUSION

The work in this article has proposed a multivariable supervisor of electric power generation units connected to high voltage power systems. A methodology has been developed to build the strategy for the supervision of these power generation units. This is based on artificial neural networks. The simulation results showed that this ANN supervisor was able to participate in the secondary frequency control for the electric power generation units connected to the interconnected power system. Future work will focus on real-time experimental validation.

ACKNOWLEDGMENT

This publication is the result of research works carried out at the Doctoral School in Sciences and Techniques of Engineering and Innovation (ED-STII) of the University of Antananarivo, Madagascar. The corresponding author would like to thank Prof. Paul A. Randriamitantsoa, Director of the ED-STII, for having welcomed him to this Doctoral School. In particular, he would like to thank Prof. Elisée Rastefano, Thesis Director, and Edmond Randriamora Co-Director, for their supervision, advice and encouragement.

REFERENCES

[1]. Negenborn. R.R, Beccuti. A.G, Demiray. T, Leirens. S, Damm. G, De Schutter. B and Morari. M, (2007). "Supervisory hybrid model predictive control for voltage stability of power networks," Proceedings of the 2007 American Control Conference, New York City, July 11-13, 2007, pp. 5444-5449.

[2]. Negenborn. R.R, Leirens. S, De Schutter. B and Hellendoorn. J, (2009). "Supervisory nonlinear MPC for emergency voltage control using pattern search," Control Engineering Practice, Vol 7, July 2009, pp.841-848.

[3]. Qi. W, Liu. J, Chen. X and Christofides. P, (2011), "Supervisory Predictive Control of Standalone Wind-Solar Energy Generation Systems," IEEE Transactions on Control Systems Technology, Vol. 19. No 1, January 2011, pp. 199-207.

[4]. Tedesco. F, Mariam. L, Basu. M, Casavola. A and Conlon. M.F, (2016). "Supervision of Community Based Microgrids: an Economic Model Predictive Control Approach," International Conference on Renewable Energies and Power Quality (ICPREQ'16), Madrid, 4-6 May, 2016, pp. 172-177.

[5]. Courtecuisse. V, Breban. S, Nasser. M, Vergnol. A, Robyns. B and Radulescu. M, (2007). "Supervision d'une centrale multisources basée sur l'association éolien, microhydraulique et stockage d'énergie," Electrotechnique du future 2007, 07 Septembre – Toulouse - France, pp. 1-8.

[6]. Boukettaya. G, Krichen. L and Ouali. A, (2007). "Fuzzy Logic Supervisor for Power Control of an Isolated Hybrid Energy Production Unit," International Journal of Electrical and Power Engineering 1 (3) 279-285, 2007.

[7]. Herbreteau. J, Coutercuisse. V, Degobert. P, Robyns. B and François. B, (2008).

"Association of PV, gas microturbine and short term storage system to participate in frequency control," 8th International Conference on Renewable Energies and Power Quality (ICREPQ), Vol 1. No 6, March 2008, pp. 358-363.

[8]. Li. P, Degobert. P, Robyns. B and François. B, (2009). "Participation in the Frequency Regulation Control of a Resilient Microgrid for a Distribution Network," International Journal of Integrated Energy Systems, Vol. 1, No 1, January-June 2009, pp. 1-5.

[9]. Nasser. M, Vergnol. A and Robyns. B, (2011). "Supervision for wind-hydro power plant and storage system connected to AC grid," MIXGENERA 2011, November 17, 2011.

[10]. Shabib. G, (2012). "Applications of Supervisory PID Controller to a Power System," International Journal of Control Science and Engineering 2012, 2(5):102-110.

[11]. Ngoffe. S.P, Imano. A.M, and Essiane .S.N, (2016). "Optimisation d'un superviseur flou par la méthode des couloirs : Application à la supervision d'un système Photovoltaïque-Diesel," Symposium de Génie Electrique, 7-9 juin 2016, Grenoble, France.

[12]. Krim. Y, Abbes. D, Krim. S and Mimouni. M.F, (2017). "Control and Fuzzy Logic Supervision of a Wind Power System with Battery-Supercapacitor Hybrid Energy Storage," 14th International Workshop on Advanced Control and Diagnosis, 16-17 November 2017, Bucharest, Romania.

[13]. Roumila. Z, Rekioua. D and Rekioua T, (2017). "Energy management based fuzzy logic controller of hybrid system wind-photovoltaic-Diesel with storage battery," International Journal of Hydrogen Energy, 42 (2017) 19525-19535.

[14]. Chaouali. H, Ben Salem. W, Mezghani. D and Mami. A, (2018). "Fuzzy Logic Optimization of a Centralized Energy Management Strategy for a Hybrid PV-PEMFC System Feeding a Water Pumping Station," International Journal of Renewable Energy Research, Vol.8, No.4, December, 2018, pp. 2190-2198.

[15]. Mohagheghi. S, Venayagamoorthy. G.K and Harley. RG, (2005). "A Dynamic Recurrent Neural Network for Wide Area Identification of a Multimachine Power System with a FACTS Device," Proceeding of the IEEE International Joint Conference on Neural Networks, 2005, pp.215-220.

[16]. Younsi. S, Jraidi. M, Hamrouni. N and Cherif. A, (2011). "Artificial Neural Networks Control of Hybrid Renewable Energy System Connected to AC Grid," International Journal of Computational Intelligence Technique, Vol 2, Issue 2, 2011, pp. 44-52.

[17]. Lu. N, (2019). "An Artificial Neural Network-Based Frequency Nadir Estimation Approach for Distributed Virtual Inertia Control,".

[18]. Morovati. S and Pulgar-Painemal. H, (2021). "Control coordination between DFIG-based wind turbines and synchronous generators for optimal primary frequency response," 52th North American Power Symposium (NAPS).

[19]. Ramanantena. G, (2018). "Conception et étude de fonctionnement du réseau interconnecté. Cas du réseau de la région DIANA," Mémoire de Master of Research, Université d'Antananarivo.

[20]. Craciun. D.I, (2010). "Modélisation des équivalents dynamiques des réseaux électriques," Ph.D Dissertation, université de Grenoble.

[21]. Lal. D.K and Barisal. A.K, (2019). "Combined Load Frequency and Terminal Voltage Control of Power Systems using Moth-flame Optimization Algorithm," Journal of Electrical System an Information Technology (JESIT), vol. 6, n°8, December 2019, pp. 1-24.

[22]. Zabaiou. T, (2005). "Compensation des délais de communication d'une commande globale de réseau électrique," Mémoire de Maîtrise, Université de Québec.

[23]. Benhamed .S, Ibrahim. H, Belmokthar. K, Hosni. H, Ilinca. A, Rousse. D, Chandra. A and Ramdenee. D, (2016). "Dynamic Modeling of Diesel Generator Based on Electrical and Mechanical Aspects," 2016 IEEE Electrical Power and Energy Conference (EPEC), 08 December 2016.

[24]. Siddiqui. M.K, Mallick. M.A and Iqbal. A, (2019). "Performance Analysis of Closed Loop Control of Diesel Generator Power Supply for Base Transceiver Load," International Journal of Innovative Technology and Exploring Engineering (IJITEE), Volume-8 Issue-9, July 2019, pp. 2483-2495.

[25]. Arantzamendi. H.G, (2006). "Etude de structures d'intégration de génération décentralisée : Application aux

microréseaux," Ph.D Dissertation, Institut National Polytechnique de Grenoble.

[26]. Thirault. D, (2004). "Architectures des réseaux de distribution pour l'électrification rurale des pays en développement," Ph.D Dissertation, Institut National Polytechnique de Grenoble.

[27]. Teninge. A, (2009). "Participation aux services système de parcs éoliens mixtes," Ph.D Dissertation, Institut National Polytechnique de Grenoble.

[28]. Tameche. T.A.T, (2012). "Modélisation et simulation d'un système de jumelage Eolien-Diesel alimentant une charge locale," Mémoire de Maîtrise, Université de Québec.

[29]. Ramanantena. G, Andriamahatana. T.L and Andrianaharison. Y, (2021). "Design of a Neural Supervisor of Electrical Energy Production Units," International Journal of Engineering Research and Management (IJERM), Volume-08, Issue-03, March 2021, pp. 1-5.

[30]. Ramanantena. G and Andrianaharison. Y.D, (2021). "Design of a Supervision of the Electric Power Generation Units by a Multivariable Neural System," Journal of Scientific and Engineering Research (JSAER), Volume-08, Issue-03, March 2021, pp. 84-92.